ChemComm

COMMUNICATION

View Article Online
View Journal

Cite this: DOI: 10.1039/d4cc03767g

Received 29th October 2024,
Accepted 29th November 2024

DOI: 10.1039/d4cc03767g

rsc.li/chemcomm

Non-toxic core–shell nanowires for *in vitro* extracellular vesicle scavenging†

Piyawan Paisrisarn,[a] Kunanon Chattrairat,[*b] Yuta Nakamura,[a] Kazuki Nagashima,[c] Takeshi Yanagida,[d] Yoshinobu Baba[*aef] and Takao Yasui[*bef]

Extracellular vesicles (EVs) from cancer cells promote abnormal growth in normal cells, potentially leading to cancer proliferation. We developed a nanowire-based EV-elimination device that efficiently eliminated EVs without toxicity. This method restored normal growth in mammary gland cells cultured with breast adenocarcinoma-derived EVs containing medium treated with the device.

Extracellular vesicles (EVs) are phospholipid bilayer-enclosed structures ranging in size from 40–1000 nm that have been identified in various biofluids, such as serum, urine, saliva, and tears, where they may indicate the presence, development, and therapeutic response of various diseases.[1] Recently, EVs have been recognized as some of the most promising liquid biopsy biomarkers that are involved in numerous *in vivo* phenomena, including intercellular communication and disease progression. The EVs play an essential role in the proliferation and metastasis of cancers *via* miRNAs and proteins contained in EVs. Previous studies have reported that EVs are involved in the propagation and spread of disease-associated regulators to distant cells through the blood vessels and lymph, leading to metastasis and causing death.[2]

EVs secreted from cancer cells are involved in tumor initiation, progression, metastasis, and chemotherapy resistance by their ability to carry oncogenesis RNAs and proteins.[3] Metastasis *in vitro* is characterized by the presence of abnormal and pathogenic EVs that can induce abnormal cell growth of specific normal cells and lead to cancer development. The EV formation is largely regulated by the endosomal sorting complex required for transport (ESCRT) pathway and is controlled by the sphingomyelinase family.[1] Inhibition of EV secretion by knockdown of many key proteins, such as the ESCRT machinery and Rab proteins, is an alternative therapy method; however, this method tends to cause embryonic lethality in mammals.[4] Because EVs play an important role in the pathogenesis of diseases, EV elimination is required.

A device designed to eliminate EVs is a potential candidate for purifying biofluids to suppress cancer metastasis and proliferation, particularly when EVs are recognized as pathogens under cancerous physiological and pathological conditions.[3] A well-known example of biofluid purification is blood purification devices, which are used to remove pathogens from patients' blood, including those causing sepsis.[5] Based on this concept, we came up with the idea of removing EVs from patients' blood. To capture EVs from biological samples such as blood, serum, and urine, we demonstrated the potential of nanowire-based technology as a promising tool.[6–13] Our present study was inspired by the combination of nanowire-based technology and blood purification devices to remove EVs in patients, similar to the role of these devices in eliminating sepsis-causing pathogens. As the first step toward the long-term goal of developing a nanowire-based purification device, we fabricated an EV-elimination device to eliminate EVs from the cancer cell culture media.

As EVs derived from cancer cells are involved in metastasis through their circulation *via* blood vessels and they regulate abnormal cell growth in normal cells, we used a cell proliferation assay to evaluate our EV-elimination device (Fig. 1). First, we collected media containing EVs derived from the MDA-MB-231 cell line, which is a breast cancer cell line. Then, we observed cell proliferation by culturing MCF10A cells, which are a human mammary epithelial cell line, in media not containing EVs (called the no EV media), in media containing EVs, and in recovered media obtained by using the EV-elimination device.

[a] *Department of Biomolecular Engineering, Graduate School of Engineering, Nagoya University, Furo-cho, Chikusa-ku, Nagoya 464-8603, Japan*
[b] *Department of Life Science and Technology, Institute of Science Tokyo, Nagatsuta 4259, Midori-ku, Yokohama 226-8501, Japan. E-mail: chattrairat.k.0716@m.isct.ac.jp, yasuit@life.isct.ac.jp*
[c] *Research Institute for Electronic Science (RIES), Hokkaido University, Kita, Sapporo, Hokkaido 001-0020, Japan*
[d] *Department of Applied Chemistry, Graduate School of Engineering, The University of Tokyo, 7-3-1 Hongo, Bunkyo-ku, Tokyo 113-8656, Japan*
[e] *Institute of Quantum Life Science, National Institutes for Quantum Science and Technology (QST), Anagawa 4-9-1, Inage-ku, Chiba 263-8555, Japan. E-mail: baba.yoshinobu@qst.go.jp*
[f] *Research Institute for Quantum and Chemical Innovation, Institutes of Innovation for Future Society, Nagoya University, Furo-cho, Chikusa-ku, Nagoya 464-8603, Japan*

† Electronic supplementary information (ESI) available: Materials and methods, Fig. S1–S10, and Table S1. See DOI: https://doi.org/10.1039/d4cc03767g

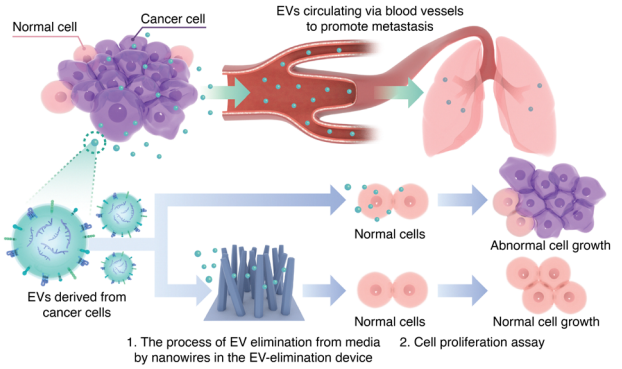

Fig. 1 Schematic illustration of a model cancer metastasis by EVs and elimination of EVs by using our EV-elimination device. The cancer cells secret EVs that circulate *via* blood vessels to promote metastasis. We confirmed that when culturing normal cells with the EVs derived from the cancer cells, abnormal cell growth would occur. This in turn suggested that the EVs could induce abnormal cell growth in normal cells. We developed the EV-elimination device to eliminate the cancer-derived EVs from the media and used the recovered media to culture normal cells. The proliferation degree of normal cells cultured with the recovered media indicated normal cell growth, and it implied that successful EV elimination was achieved.

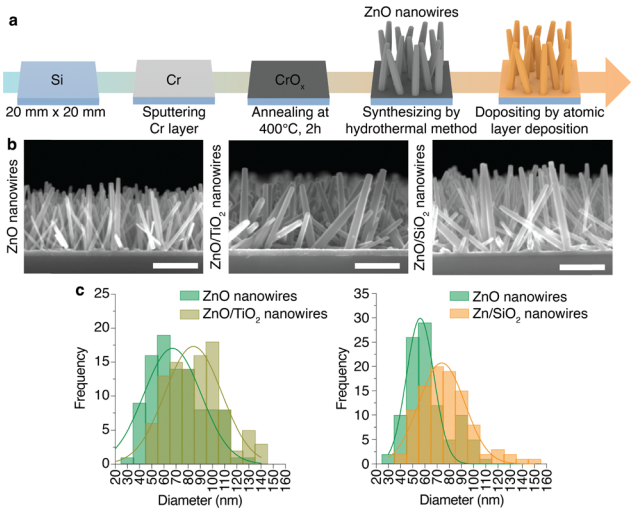

Fig. 2 Metal oxide nanowire fabrication and characterization. (a) ZnO nanowires were synthesized by a hydrothermal method on a silicon substrate having a sputtered chromium (Cr) layer, and the TiO_2 and SiO_2 layers were deposited on ZnO nanowires by ALD. (b) FESEM images and (c) the histograms of nanowire diameter comparing ZnO nanowires before and after depositing TiO_2 or SiO_2 layers. Lines indicate the fitting Gaussian distribution (n = 100 nanowires).

Finally, we compared the proliferation of normal cells by culturing them with media containing cancer cell-derived EVs and with recovered media from the EV-elimination device.

We fabricated the EV-elimination device with three different materials for the nanowires to provide different charged surfaces.[14] In addition to bare zinc oxide (ZnO) nanowires, we fabricated ZnO nanowires with a titanium dioxide (TiO_2) layer and ZnO nanowires with a silicon dioxide (SiO_2) layer obtained by an atomic layer deposition (ALD) technique and designated as ZnO/TiO_2 (core/shell) and ZnO/SiO_2 (core/shell) nanowires, respectively (Fig. 2a).[15] The average height of the bare ZnO, ZnO/TiO_2 (core/shell), and ZnO/SiO_2 (core/shell) nanowires was about 1.4 μm (n = 60) (Fig. 2b). The morphology of a single nanowire of each type was obtained using scanning transmission electron microscopy (STEM) (Fig. S1, ESI†). The average diameters of the ZnO, ZnO/TiO_2 (core/shell), and ZnO/SiO_2 (core/shell) nanowires were 66.34, 86.90, and 77.64 nm, respectively. The diameter size distribution of the ZnO/TiO_2 (core/shell) and ZnO/SiO_2 (core/shell) nanowires was shifted to larger diameters by about 15 nm compared to the bare nanowires, which indicated that the oxide layer using ALD was successfully realized (Fig. 2c). After placing the substrate with ZnO, ZnO/TiO_2 (core/shell), and ZnO/SiO_2 (core/shell) nanowires inside the assembled Teflon block,[8] we fabricated the EV-elimination device.

The ZnO, ZnO/TiO_2 (core/shell), and ZnO/SiO_2 (core/shell) nanowires eliminated EVs by different interactions and they eliminated different EV sub-populations. First, we obtained ultracentrifuged EVs from the MDA-MB-231 cells with zeta potential and average size of −22.5 mV and 140 nm, respectively (Fig. 3a and b). The ultracentrifuged EVs were dispersed in PBS, incubation of PBS was carried out in the block, and the metal oxide nanowires eliminated the EVs from the PBS. The elimination efficiencies were calculated using the $(C_0–C_r)/C_0$ equation where C_0 is the initial EV concentration and C_r is the remaining EV concentration after incubation in the EV-elimination device. The ZnO nanowires eliminated EVs with the highest efficiency, followed by ZnO/TiO_2 (core/shell) and ZnO/SiO_2 (core/shell) nanowires (Fig. 3c). Moreover, the results showed that a longer incubation time resulted in higher elimination efficiency, and that suggested a longer incubation time made it possible to capture a greater number of EVs on the nanowires. We previously found that the electrostatic interaction and hydrogen bonding between EVs and nanowires play important roles in the EV capture mechanism,[11,12,14] and from that we suggested different elimination efficiencies and different EV sub-populations were eliminated due to the different zeta potential of EV sub-populations. Because we used PBS of pH 7.2 for EV collection and incubation, the surface charge of the ZnO nanowires was positive due to their isoelectric point of ~9.5, whereas the surface charges of the ZnO/TiO_2 (core/shell) and ZnO/SiO_2 (core/shell) nanowires were negative due to their isoelectric points of ~5.2 and ~3.9, respectively.[15] Because of

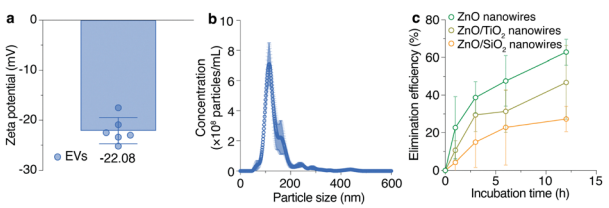

Fig. 3 EV characterization and elimination efficiency of the EV-elimination device. (a) Zeta potential of EVs. Data represent mean ± standard deviation (n = 6). (b) Size distribution of EVs. Data represent mean ± standard deviation (n = 3). (c) Elimination efficiency for ZnO, ZnO/TiO_2 (core/shell), and ZnO/SiO_2 (core/shell) nanowires. Data represent mean ± standard deviation (n = 3).

the electrostatic interaction and hydrogen bonding, the negatively charged EVs easily interacted with positively charged surfaces, *i.e.*, the ZnO nanowires, rather than the negatively charged surfaces, *i.e.*, ZnO/TiO_2 (core/shell) and ZnO/SiO_2 (core/shell) nanowires, leading to different elimination efficiencies (Fig. 3c and Fig. S2, ESI†).[8]

We found a critical condition that promoted the abnormal proliferation degree when culturing MCF10A cells with MDA-MB-231 cell-derived EVs by experimentally varying the conditions, including the components of the cell culture media, cell passage number, cell seeding condition, and EV concentration (Fig. 4a and Fig. S3, ESI†). By comparing the proliferation degree with and without the EVs, we defined abnormal cell growth as having occurred when the p value was less than 0.01 in a statistical analysis by a two-tailed t-test. We found that MCF10A cells cultured in mammary epithelial cell growth basal medium (MEBM) at passage number 5 (P5) with 5000 seeding cells/well and 10^8 to 10^9 EV particles per mL had the highest proliferation degree (Fig. S3, ESI†). Although we used EVs from only one cell line, MDA-MB-231, the number of EVs affected cell proliferation (Fig. 4a and Fig. S4, ESI†). We also compared the cell proliferation degree between the conditions with and without EVs and found that adding 10^9 EV particles per mL resulted in a significant increase in abnormal cell growth, with an abnormal cell growth ratio of 2 (Fig. S5, ESI†). The growth ratio of 2 indicated that the proliferation under each condition was twice as high as that under the no-EV condition. From these results, we decided that the critical concentration of EVs to induce an abnormal proliferation degree was likely to be about 10^9 particles per mL. Although both type and number of EVs have been assumed to cause abnormal cell growth,[4] our results confirmed that the EV concentration affected the proliferation degree, possibly leading to cancer metastasis.

In addition to proliferation degree measurements, we used fluorescence localization of EVs from MDA-MB-231 cells cultured in MCF10A cells to confirm that EVs existed inside the MCF10A cells (Fig. 4b). The fluorescence images demonstrated that the EVs were inside the cytoplasm of the MCF10A cells that were labeled by the PKH26 red fluorescent dye. The compositions of EVs are recognized to induce and mediate the recipient cells, including proteins, miRNAs, and DNAs; thus, numerous research studies have presented the potential of EVs to serve as a biomarker for homeostasis and disease diagnostics. Therefore, we also investigated the EV miRNAs using the next-generation sequencing technique (Fig. 4c). We filtered miRNAs according to their expression levels and obtained 57 miRNAs using $|\log_2(\text{fold change})| \leq 5$ for repeated experiments (n = 2). Then, we sorted the miRNA expression levels from high to low and identified the top 10 miRNA expression levels. After identifying and matching these miRNAs with tumor-related functions (Table S1, ESI†), we found that six miRNAs were oncogenesis miRNAs. Oncogenesis miRNAs are involved in abnormal cell growth, leading to cancer metastasis. Better techniques to extract the miRNAs from specific sources inside or outside EVs will make precise miRNA recognition possible.[16] However, our results confirmed that the EVs from cancer cells could induce and mediate abnormal cell growth in recipient cells that are normal cells.

We evaluated the ability of metal oxide nanowires to suppress cancer metastasis using a cell proliferation assay (Fig. 5). We measured the proliferation degrees of MCF10A cells cultured in no EV media or in the recovered media after incubating in the EV-elimination device containing ZnO nanowires (Fig. 5a and Fig. S6, ESI†). We found that 10^9 EV particles per mL in the media increased the proliferation degree of MCF10A cells with statistical significance compared with the no EV media, suggesting abnormal cell growth. In addition to the increase in the proliferation degree of MCF10A cells, we also found that the ratio of proliferation degree was higher than 2 (Fig. S7, ESI†). The ZnO nanowires eliminated the EVs from MDA-MB-231 cells in the media, resulting in no proliferation degree of MCF10A cells when culturing in the recovered media after incubating 10^9 EV particles per mL in the EV-elimination device containing the ZnO nanowires. However, we also obtained no proliferation degree for the cultured MCF10A cells in the recovered media from the no EV media incubated in the EV-elimination device containing the ZnO nanowires (Fig. 5a

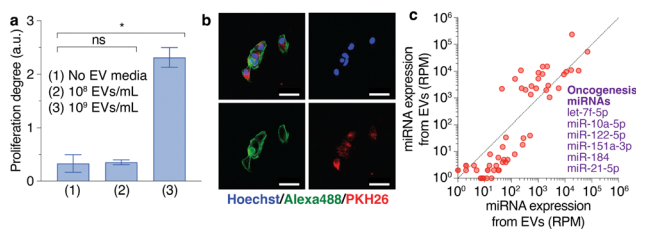

Fig. 4 Inhibition of cancer metastasis by using the EV-elimination device. (a) Cell proliferation of MCF10A cells cultured with and without EVs in media. Data represent mean ± standard deviation (n = 3) and the p values were calculated by a two-tailed t-test (*, $p < 0.01$; ns, not significant). (b) The fluorescence microscopy images show the MCF10A cells after culturing with EVs from MDA-MB-231 cells. The MCF10A cells were stained using Hoechst 33 342 blue fluorescent dye for the nuclei and the Alexa 488 green fluorescent dye for the cytoskeletons. The EVs were stained using PKH26 red fluorescent dye. The scale bars are 50 μm. (c) The scatter plot of miRNA expression levels of EVs from MDA-MB-231 cells for repeated experiments (n = 2) and the identified oncogenesis miRNAs.

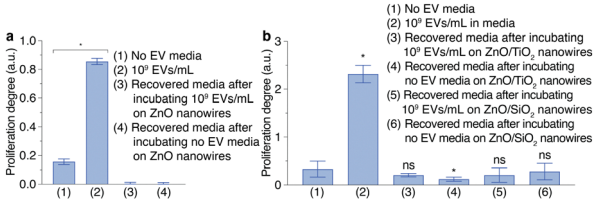

Fig. 5 Inhibition of cancer metastasis by using the EV-elimination device. (a) Cell proliferation of MCF10A cells as a comparison between culturing with no EV media and culturing with the recovered media after incubating on ZnO nanowires. Data represent mean ± standard deviation (n = 3) and the p value was calculated by a two-tailed t-test (*, $p < 0.01$). (b) Cell proliferation of MCF10A cells as a comparison between culturing with no EV media and the recovered media after incubating on ZnO/TiO_2 (core/shell) or ZnO/SiO_2 (core/shell) nanowires. Data represent mean ± standard deviation (n = 3) and the p values were calculated by comparing with the no EV media condition by a two-tailed t-test (*, $p < 0.01$; ns, not significant).

and Fig. S7, ESI†). This result confirmed that the ZnO nanowires dissolved and released Zn^{2+} ions, which affected cell proliferation and caused cell death (Fig. S6, ESI†).[17]

Then, we also measured the proliferation degree of MCF10A cells after culturing with the media recovered from a device containing ZnO/TiO_2 (core/shell) or ZnO/SiO_2 (core/shell) nanowires (Fig. 5b and Fig. S8, ESI†). As we expected, 10^9 EV particles per mL in media increased the proliferation degree and its ratio (Fig. 5b and Fig. S5, ESI†). The proliferation degrees of MCF10A cells were similar when culturing between the no EV media and the recovered media after incubating 10^9 EV particles per mL in the EV-elimination device containing ZnO/TiO_2 (core/shell) or ZnO/SiO_2 (core/shell) nanowires. These media also showed proliferation ratios lower than 2, implying that both types of nanowires eliminated the EVs from the media (Fig. S9, ESI†). However, the recovered media from the no EV media incubated in the EV-elimination device containing ZnO/TiO_2 (core/shell) nanowires lowered the proliferation degree with statistical significance, implying low toxicity (Fig. 5b). On the other hand, the recovered media from the no EV media incubated in the EV-elimination device containing ZnO/SiO_2 (core/shell) nanowires did not affect the proliferation degree of MCF10A cells. We judged that the EV-elimination device employing the ZnO/SiO_2 (core/shell) nanowires was the most suitable for future blood purification devices among the three types of nanowires that we studied. These results indicated that the recovered media from EV-elimination devices had an EV concentration below the critical threshold that could induce abnormal cell growth. Hence, the EV-elimination device inhibited abnormal cell growth by eliminating cancer-derived EVs, leading to reduction of cancer metastasis.

In this study, we fabricated ZnO, ZnO/TiO_2 (core/shell), and ZnO/SiO_2 (core/shell) nanowires and found that ZnO/SiO_2 (core/shell) nanowires showed the ability to eliminate EVs, leading to suppressing abnormal cell growth without causing cell death. Regarding device upscale, the device can be developed as a nanowire-based microfluidics device that can realize continuous flow of the solution; thus, the device has the potential to increase future purification applications from microliter amounts up to milliliter amounts. Furthermore, the nanowire surfaces can be modified with antibodies to capture specific EVs,[10] suppressing non-specific capture of such things as blood cells and proteins. We took the first step by preparing an EV-elimination device for the final goal of developing a nanowire-based purification device to administer cancer therapies, inhibit metastases, and provide new therapeutic strategies.

This research was supported by the Japan Agency for Medical Research and Development (AMED) Grant no. JP21he2302007, the Moonshot Research and Development Program (Grant no. 22zf0127004s0902 and JP22zf0127009) from the AMED, the New Energy and Industrial Technology Development Organization (NEDO) JPNP20004, the Japan Science and Technology Agency (JST) AIP Acceleration Research (JPMJCR23U1), and the JSPS Grant-in-Aid for Scientific Research (A) 24H00792. For their valuable discussions, we especially thank Dr H. Yukawa, Dr D. Onoshima, Dr T. Shimada and Dr A. Arima.

Data availability

The data supporting this article have been included as part of the ESI.†

Conflicts of interest

There are no conflicts to declare.

Notes and references

1 G. van Niel, G. D'Angelo and G. Raposo, *Nat. Rev. Mol. Cell Biol.*, 2018, **19**, 213–228.
2 A. H. Buck, G. Coakley, F. Simbari, H. J. McSorley, J. F. Quintana, T. Le Bihan, S. Kumar, C. Abreu-Goodger, M. Lear, Y. Harcus, A. Ceroni, S. A. Babayan, M. Blaxter, A. Ivens and R. M. Maizels, *Nat. Commun.*, 2014, **5**, 5488.
3 C. P. R. Xavier, H. R. Caires, M. A. G. Barbosa, R. Bergantim, J. E. Guimaraes and M. H. Vasconcelos, *Cells*, 2020, **9**, 1141.
4 A. G. Yates, R. C. Pink, U. Erdbrugger, P. R. Siljander, E. R. Dellar, P. Pantazi, N. Akbar, W. R. Cooke, M. Vatish, E. Dias-Neto, D. C. Anthony and Y. Couch, *J. Extracell. Vesicles*, 2022, **11**, e12151.
5 J. H. Kang, M. Super, C. W. Yung, R. M. Cooper, K. Domansky, A. R. Graveline, T. Mammoto, J. B. Berthet, H. Tobin, M. J. Cartwright, A. L. Watters, M. Rottman, A. Waterhouse, A. Mammoto, N. Gamini, M. J. Rodas, A. Kole, A. Jiang, T. M. Valentin, A. Diaz, K. Takahashi and D. E. Ingber, *Nat. Med.*, 2014, **20**, 1211–1216.
6 T. Yasui, T. Yanagida, S. Ito, Y. Konakade, D. Takeshita, T. Naganawa, K. Nagashima, T. Shimada, N. Kaji, Y. Nakamura, I. A. Thiodorus, Y. He, S. Rahong, M. Kanai, H. Yukawa, T. Ochiya, T. Kawai and Y. Baba, *Sci. Adv.*, 2017, **3**, e1701133.
7 Y. Kitano, K. Aoki, F. Ohka, S. Yamazaki, K. Motomura, K. Tanahashi, M. Hirano, T. Naganawa, M. Iida, Y. Shiraki, T. Nishikawa, H. Shimizu, J. Yamaguchi, S. Maeda, H. Suzuki, T. Wakabayashi, Y. Baba, T. Yasui and A. Natsume, *ACS Appl. Mater. Interfaces*, 2021, **13**, 17316–17329.
8 T. Yasui, P. Paisrisarn, T. Yanagida, Y. Konakade, Y. Nakamura, K. Nagashima, M. Musa, I. A. Thiodorus, H. Takahashi, T. Naganawa, T. Shimada, N. Kaji, T. Ochiya, T. Kawai and Y. Baba, *Biosens. Bioelectron.*, 2021, **194**, 113589.
9 P. Paisrisarn, T. Yasui, Z. Zhu, A. Klamchuen, P. Kasamechonchung, T. Wutikhun, V. Yordsri and Y. Baba, *Nanoscale*, 2022, **14**, 4484–4494.
10 A. Yokoi, M. Ukai, T. Yasui, Y. Inokuma, K. Hyeon-Deuk, J. Matsuzaki, K. Yoshida, M. Kitagawa, K. Chattrairat, M. Iida, T. Shimada, Y. Manabe, I.-Y. Chang, E. Asano-Inami, Y. Koya, A. Nawa, K. Nakamura, T. Kiyono, T. Kato, A. Hirakawa, Y. Yoshioka, T. Ochiya, T. Hasegawa, Y. Baba, Y. Yamamoto and H. Kajiyama, *Sci. Adv.*, 2023, **9**, eade6958.
11 K. Chattrairat, T. Yasui, S. Suzuki, A. Natsume, K. Nagashima, M. Iida, M. Zhang, T. Shimada, A. Kato, K. Aoki, F. Ohka, S. Yamazaki, T. Yanagida and Y. Baba, *ACS Nano*, 2023, **17**, 2235–2244.
12 K. Chattrairat, A. Yokoi, M. Zhang, M. Iida, K. Yoshida, M. Kitagawa, A. Niwa, M. Maeki, T. Hasegawa, T. Yokoyama, Y. Tanaka, Y. Miyazaki, W. Shinoda, M. Tokeshi, K. Nagashima, T. Yanagida, H. Kajiyama, Y. Baba and T. Yasui, *Device*, 2024, **2**, 100363.
13 M. Zhang, M. Ono, S. Kawaguchi, M. Iida, K. Chattrairat, Z. Zhu, K. Nagashima, T. Yanagida, J. Yamaguchi, H. Nishikawa, A. Natsume, Y. Baba and T. Yasui, *ACS Appl. Mater. Interfaces*, 2024, **16**, 29570–29580.
14 T. Yasui, P. Paisrisarn, T. Yanagida, Y. Konakade, Y. Nakamura, K. Nagashima, M. Musa, I. A. Thiodorus, H. Takahashi, T. Naganawa, T. Shimada, N. Kaji, T. Ochiya, T. Kawai and Y. Baba, *Biosens. Bioelectron.*, 2021, **194**, 113589.
15 M. Musa, T. Yasui, Z. Zhu, K. Nagashima, M. Ono, Q. Liu, H. Takahashi, T. Shimada, A. Arima, T. Yanagida and Y. Baba, *Anal. Sci.*, 2021, **37**, 1139–1145.
16 D. K. Jeppesen, A. M. Fenix, J. L. Franklin, J. N. Higginbotham, Q. Zhang, L. J. Zimmerman, D. C. Liebler, J. Ping, Q. Liu, R. Evans, W. H. Fissell, J. G. Patton, L. H. Rome, D. T. Burnette and R. J. Coffey, *Cell*, 2019, **177**(428–445), e418.
17 A. R. Pinho, F. Martins, M. E. V. Costa, A. M. R. Senos, O. Silva, M. L. Pereira and S. Rebelo, *Cells*, 2020, **9**, 1081.

